



Published in final edited form as:

Nanomedicine (Lond). 2012 March ; 7(3): 429–445. doi:10.2217/nmm.12.12.

Advances in molecular imaging: targeted optical contrast agents for cancer diagnostics

Anne Hellebust and Rebecca Richards-Kortum*

Rice University, Bioengineering Department, 6100 Main Street, Bioengineering, MS 142, Houston, TX 77005-1892, USA

Abstract

Over the last three decades, our understanding of the molecular changes associated with cancer development and progression has advanced greatly. This has led to new cancer therapeutics targeted against specific molecular pathways; such therapies show great promise to reduce mortality, in part by enabling physicians to tailor therapy for patients based on a molecular profile of their tumor. Unfortunately, the tools for definitive cancer diagnosis – light microscopic examination of biopsied tissue stained with nonspecific dyes – remain focused on the analysis of tissue *ex vivo*. There is an important need for new clinical tools to support the molecular diagnosis of cancer. Optical molecular imaging is emerging as a technique to help meet this need. Targeted, optically active contrast agents can specifically label extra- and intracellular biomarkers of cancer. Optical images can be acquired in real time with high spatial resolution to image-specific molecular targets, while still providing morphologic context. This article reviews recent advances in optical molecular imaging, highlighting the advances in technology required to improve early cancer detection, guide selection of targeted therapy and rapidly evaluate therapeutic efficacy.

Keywords

biomarkers; cancer; contrast agents; early diagnosis; image-guided therapeutics; nanoparticles; optical imaging

Background

Importance of early detection

Cancer is an important global public health challenge. More than a third of Americans will be diagnosed with cancer at some time in their lives, and costs of cancer in the USA exceeded US\$219 billion in 2008 [201]. Globally, the number of deaths due to cancer will double in the next 20 years [202]. Improving global efforts to detect cancer at an early stage is one of the most important strategies to reduce morbidity and mortality of cancer worldwide, as defined by the National Cancer Institute [203]. Detecting and treating cancer before metastasis improves the odds of survival; when detected late, cancer treatment is less effective, has greater morbidity and is more expensive.

© 2012 Future Medicine Ltd

*Author for correspondence: Tel.: +1 713 348 3022; +1 713 348 3823, Fax: +1 713 348 5877, rkortum@rice.edu.

Financial & competing interests disclosure

The authors have no other relevant affiliations or financial involvement with any organization or entity with a financial interest in or financial conflict with the subject matter or materials discussed in the manuscript apart from those disclosed.

No writing assistance was utilized in the production of this manuscript.

There are more than 10,000,000 malignancies diagnosed each year, of which 80% arise on epithelial surfaces. Such cancers, including those in the oral cavity, oropharynx and esophagus, are associated with poor survival, primarily due to diagnosis at a late, incurable stage. While visual screening and biopsy are recommended for atrisk individuals, the standard white-light exam frequently misses areas of early neoplasia; for example, endoscopic screening for esophageal cancer in individuals with Barrett's esophagus is known to miss up to 48% of early cancers [1]. Moreover, incomplete resection leads to frequent recurrence. There is a need for new imaging tools to improve early diagnosis and to guide effective treatment. However, the benefits of improved screening must be balanced against the potential harms associated with early detection of cancers that may have remained indolent [2]. There is an urgent need for molecular imaging tools that can help identify those lesions with greatest risk of progression.

Role of molecular imaging in early-stage neoplasia

Many features of the neoplastic process [3] can be visualized using molecular imaging [4], including changes in gene expression, the expression of cell surface receptors, changes in epithelial–stromal communication (e.g., signaling associated with epithelial migration and invasion) [5] and epithelial cell apoptosis. PET and MRI have shown promise for molecular imaging of cancer [6], and 2-deoxy-2-¹⁸F-fluoro-D-glucose PET imaging is now used routinely to assess the response of solid tumors to therapy. However, PET and MRI are too expensive for population-based screening [7], and often require intravenous (iv.) injection of contrast agent, which is impractical in low-risk populations.

Developing tools to quantitatively image multiple biomarkers, at multiple spatial resolution scales, across the entire epithelial surface at risk would have many important clinical advantages. First, such tools could facilitate detection of precancerous lesions at a time when treatment is most effective. Second, image-guided resection could enable more complete resection of early disease. Finally, such techniques could change the future practice of molecular therapeutics, by helping to select the most appropriate choice of therapeutic agent and providing a rapid molecular and cellular assessment of response. This is particularly significant, given the increasing use of monoclonal antibody-based therapies, such as cetuximab, bevacizumab and trastuzumab. As our identification, understanding and ability to target new biomarkers related to neoplastic progression improves, better methods for *in vivo* phenotyping of tumors are necessary.

Optical molecular imaging

Optical molecular imaging systems have the potential to help meet these needs; optical imaging systems can be portable, inexpensive and provide real-time images of whole organs at the macroscopic scale, with the potential to zoom in and image subcellular structures from smaller regions of interest. The chief limitation of optical imaging approaches is that they have a relatively small depth of penetration (ranging from hundreds of microns to several centimeters, depending on the approach), due to the scattering and absorption of light in tissue. Thus, while optical imaging is well suited to study surface lesions, it cannot currently be used for whole-body imaging. However, optical imaging may be combined with other modalities, such as MRI [8], yielding multimodal strategies that combine the benefits of each approach.

Endogenous optical contrast can provide information regarding angiogenesis, hypoxia, cell metabolism and invasion [9–11]. Optically active contrast agents applied topically prior to imaging can be used to visualize a broader range of molecular changes; these agents have the potential to increase image contrast between neoplastic and healthy tissue thereby facilitating the detection of cancer at the earliest possible stages. The ability to

noninvasively image the spatial and temporal distribution of multiple biomarkers across a tumor surface also has the potential to improve treatment, through better selection of targeted therapeutic agents, realtime imaging for *in situ* guidance of tumor margin assessment and monitoring patient response to treatment without the need for biopsy.

Optical molecular imaging systems consist broadly of three components: an optically active contrast agent targeting a specific biomarker of clinical relevance; a method to safely deliver the contrast agent to the tissue at risk; and an optical imaging system to acquire, process and interpret the resulting images of the labeled tissue. As these tools are low cost, portable and can be miniaturized, they are capable of expanding access to early detection and improving minimally invasive treatment in a wide variety of urban and rural healthcare settings. However, achieving the potential of this technology requires coordinated efforts in biomarker discovery and validation, design and delivery of contrast agents, and engineering of optical instrumentation. In this paper, we review recent advances in these areas, focusing on advances in imaging agents and delivery systems. More comprehensive reviews of advances in optical instrumentation may be found elsewhere [9,12]. We conclude by discussing the steps necessary to translate optical molecular imaging from a laboratory research tool to incorporation as part of routine clinical examination.

Endogenous optical contrast

Optical images carry information regarding signatures arising from endogenous and exogenous biomarkers [9,13]. The spatial resolution and field of view of optical imaging systems can be adjusted to interrogate tissue over a wide range of spatial scales; the field of view of widefield optical imaging systems can easily span tens of centimeters, while the spatial resolution of intravital optical microscopy systems can reach subcellular levels.

A number of wide-field imaging platforms designed to improve the early detection of neoplasia by imaging endogenous optical properties of tissue are being evaluated in large, multicenter clinical trials. For example, Curvers *et al.* developed a tri-modal endoscope to improve the early detection of esophageal neoplasia in patients with Barrett's esophagus. The endoscope combines three wide-field optical imaging modalities; the first two modalities, high-definition white-light endoscopy and autofluorescence imaging, serve as 'red-flag' techniques to identify potentially neoplastic lesions with high sensitivity based on atypical glandular patterns and/or loss of autofluorescence. Suspicious areas are then imaged using narrow-band reflectance imaging to enhance visualization of superficial vasculature features to improve specificity. In a multicenter study of 84 patients with Barrett's esophagus, Curvers and colleagues compared the sensitivity and specificity of each mode for diagnosis of neoplasia to the gold standard of histopathology [14]. Autofluorescence imaging raised the detection rate of neoplasia from 45 to 90% relative to high-definition white-light endoscopy; however, autofluorescence imaging was associated with a high false-positive rate. The use of narrow-band imaging reduced the false-positive rate from 81 to 26% relative to autofluorescence imaging.

Similar devices have been developed to identify early neoplastic changes in oral, cervical and pulmonary mucosa based on changes in endogenous optical properties [11,15–17]. In each organ site, neoplastic lesions are typically associated with loss of autofluorescence; areas that exhibit loss of autofluorescence are often clinically occult under traditional white-light imaging [11,17,18]. In the last few years, a number of wide-field optical imaging systems have received US FDA approval to augment early detection of neoplastic lesions, including the VELscope[®] (oral; LED Medical Diagnostics Inc., BC, Canada), Trimira[®]-3000 (oral; DentalEZ Group, PA, USA), Olympus[®] Lucera (gastrointestinal; Olympus, Tokyo, Japan) and the Xillix[™] LIFE scope (lung; Xillix Technologies Corp., BC,

Canada). Still, specificity of wide-field imaging remains a significant concern as benign changes such as inflammation can also be associated with loss of autofluorescence [14,19–21].

To address the limitations associated with endogenous contrast, a number of targeted, optically active contrast agents have been developed. These agents are generally comprised of two parts: a targeting moiety and an optically active probe (Figure 1). Targeted agents have the potential to increase image contrast between normal and neoplastic tissue and to improve the specificity of optical imaging. The targeting moiety is an important determinant of the specificity and sensitivity of the contrast agent. The targeted biomarker must be adequately abundant for detection and sufficiently specific to the particular disease or stage of the disease under examination to yield adequate image contrast. Once the target biomarker has been identified, a targeting moiety must be selected. Antibodies, antibody fragments and peptides identified from phage-display peptide libraries are some of the most commonly used targeting moieties; each class of targeting molecule is associated with different binding kinetics and delivery challenges. In each case, an optically active probe must be conjugated to the targeting moiety, often via an amine, carboxyl or thiol functional group present in the targeting protein. The optically active probe provides the ability to visualize the target in a particular imaging modality. Optical probes that have shown promise for molecular imaging include organic fluorophores, metal nanoparticles, nanoshell composites and semiconductor nanocrystals. Again, each is associated with different delivery challenges and limits of optical detection. Stability, contrast, the potential to image multiple targets and toxicity are important considerations when selecting both the targeting moiety and the optical probe. Recent advances in contrast agent design are discussed in the following sections, organized according to the type of optical probe.

Fluorescent contrast agents for molecular imaging

Organic fluorescent dyes are routinely used as contrast agents in immunohistochemical staining protocols. Owing to their low molecular weight, high quantum yield, relatively low cost and the existence of well-developed conjugation protocols, they represent an ideal optical label for molecular imaging probes. Of particular interest are dyes that fluoresce in the near-infrared (NIR) range, where tissue turbidity is lowest and the greatest depth of light penetration can be achieved [22]. Although organic fluorophore-based contrast agents have been successfully used in small animal *in vivo* studies, clinical application lags behind [23,24].

Challenges associated with organic fluorescent dyes include their propensity for photobleaching and the relatively small number that have been approved for clinical use. Another limitation is that optical images of tissues stained with fluorescent contrast agents are highly surface weighted even in the NIR, due to light attenuation in tissue; as a practical result, these agents are of most use for imaging lesions near the epithelial surface. Finally, the contrast and sensitivity that can be achieved with contrast agents incorporating organic fluorescent dyes is largely dependent on the choice of biomarker and targeting moiety. Perhaps the most significant challenge with this approach is the difficulty of achieving high target-to-background ratios. The optical signal of targeted fluorescent dyes is largely the same whether they are bound to the targeted biomarker or not; this can limit the maximum target-to-background ratio that can be achieved and can reduce the dynamic range and sensitivity of the agent.

Antibody-targeted fluorophores

Initially, researchers developing contrast agents for *in vivo* optical molecular imaging pursued the use of monoclonal antibodies as targeting moieties for organic fluorescent dyes.

This was facilitated by the growing clinical use of therapeutic antibodies targeting relevant biomarkers of cancer, as well as by the existence of straightforward protocols for conjugating fluorescent dyes to antibodies. In particular, antibodies targeting cell surface receptors overexpressed in cancer, such as EGF receptor (EGFR), HER2 and VEGF, have been explored to target optical molecular imaging agents; sensitivity and contrast have been optimized *in vitro* in cell cultures and explanted human tumors, and *in vivo* in animal models [25–27]. Fluorescently labeled cetuximab, a chimeric anti-EGFR antibody approved for the therapy of colorectal and head and neck cancers, was administered by *iv.* injection to 20 nude mice with human gastrointestinal tumor xenografts for *in vivo* optical molecular imaging and therapeutic purposes [28]. Tumor tissue was specifically stained but surrounding normal tissue had no detectable signal, suggesting this labeled therapeutic antibody has potential as a diagnostic probe. However, the imaging time window must be optimized, as the target-to-background ratio may remain high if unbound antibodies are still circulating after *iv.* injection. Studies are ongoing to document whether the fluorescence signal measured *in vivo* correlates with therapeutic response. In a similar approach, the potential diagnostic use of fluorescently labeled bevacizumab, a humanized monoclonal antibody that binds to VEGF-A, was explored following topical application in resected human tumor specimens and *iv.* administration in nude mice with human colorectal tumor xenografts [29]. Specific labeling was achieved in both model systems and could be documented using a commercially available fluorescence endoscope.

A limitation of antibody-targeted fluorescent contrast agents is the potential immunogenicity associated with the targeting moiety. Chimeric and humanized antibodies have been engineered to decrease the immunogenicity evoked by the murine antibodies initially under investigation. In addition, antibodies are large molecules (~150 kDa), and this presents barriers to tissue penetration during *iv.* administration as well as topical application. Engineered antibody fragments are smaller in size and have the potential to improve delivery while maintaining the specificity and lowering production costs [30].

Peptide-targeted fluorophores

Targeting peptides presents an attractive alternative to the use of antibodies [31]. Their small size (<10 kDa) reduces barriers to topical delivery and tumor penetration and they are less likely to elicit an immune response [32]. A number of NIR dyes are commercially available for peptide conjugation. Amine-reactive dyes are commonly used to label lysine residues, which are relatively abundant in proteins. The targeting specificity of peptides can be compromised by fluorophore labeling; thus, reaction conditions must be optimized for every agent in order to balance the trade-off between the degree of peptide labeling and retaining target specificity. Following conjugation, excess dye must be removed, typically through filtration or dialysis, to avoid nonspecific staining. Following *iv.* injection, peptides are removed rapidly through renal excretion, thereby lowering the background fluorescence but simultaneously creating a very narrow temporal window in which imaging must be performed.

The use of peptide ligands that bind cell surface receptors that are differentially expressed on cancer cells have been explored as targeting moieties for fluorescent contrast agents. For example, EGF labeled with Alexa Fluor® 647 (Molecular Probes, OR, USA) was used to image EGFR, which is overexpressed in many epithelial cancers [33]. Increased fluorescence signal was observed in neoplastic regions of excised human oral tissue. Compared with normal mucosa from the same patient, average 2.3- and 3.8-fold increases in wide-field fluorescence were observed in precancerous and neoplastic specimens, respectively. Similarly, *iv.* administered EGF labeled with Cy5.5 was observed to specifically label EGFR-positive tumors in mice [34]. Cy5.5-EGF fluorescence was blocked by preadministered unlabeled EGF and an EGFR antibody. However,

immunohistochemistry of EGF-Cy5.5-treated tumors showed activation of the EGFR signaling pathway [35]. Before EGF can be used as a diagnostic agent, downstream effects associated with ligand–receptor binding must be considered; there is concern that potential activation and upregulation of EGFR associated with ligand binding could potentially enhance cancer progression.

The development of phage display techniques to rapidly screen libraries of peptides that selectively bind a target of interest has enabled identification of novel peptide-based targeting moieties. Both cell and tissue-based screening approaches have been developed, where peptides that selectively bind neoplastic cells or tissue with minimal binding to normal cells or tissue can be identified through multiple rounds of screening without advance knowledge of a specific target biomarker. Peptides that selectively bind to colon cancer cells have been identified by multiple groups [36,37] and used as targeting ligands for fluorescent contrast agents. Phage display techniques have also been used to select a peptide sequence selective for esophageal adenocarcinoma (SNFYMPL). A fluorescent contrast agent targeted with SNFYMPL was applied topically to endoscopically resected segments of normal, benign and neoplastic esophagus; fluorescence intensity was found to increase as tissue progressed from normal to benign intestinal metaplasia to dysplasia (Figure 2) [38].

Traditional phage display techniques identify peptides that target cancer-associated antigens but are unable to eliminate peptide sequences that will ultimately fail due to *in vivo* barriers. *In vitro* phage display is unable to test peptides against physical delivery barriers, opsonization and pharmacokinetics, issues that hinder the translation of peptides to the clinic. The screening of phage libraries in living organisms after *iv.* injection identifies peptides that are able to reach and bind to the target. Kelly *et al.* demonstrated the ability of this approach to rapidly identify phage-bearing target peptides for molecular-specific imaging [39]. Similarly, *in vivo* phage display followed by a micropanning assay was used to identify a ligand specific to human PC-3 prostate carcinoma xenografts in a murine model [40]. After labeling with an NIR fluorophore, the *iv.* contrast agent yielded a tumor-to-muscle fluorescence ratio of 30 in wide-field fluorescence imaging.

The avidity of peptide-targeted contrast agents may be optimized by increasing the number of peptide targeting moieties conjugated to each optical label. Cheng *et al.* varied the number of RGD-targeting peptides conjugated to Cy5.5 dye and examined the resulting contrast agent avidity and tumor-targeting efficacy in a subcutaneous xenograft animal model. As the number of targeting peptides per dye molecule was increased from one to four, avidity improved by approximately threefold in a cell culture model. The ratio of fluorescence signal from tumor-to-normal tissue increased moderately for the Cy5.5-conjugated RGD tetramer compared with the monomer and dimer. While all three probes were visualized, the tetramer displayed the highest tumor uptake and tumor-to-background ratio up to 4 h postinjection [41]. Similarly, phage display techniques were used to identify peptides targeting a prostate biomarker, hepsin; multiple hepsin targeting peptides were conjugated to fluorescent nanoparticles in an attempt to improve avidity and pharmacokinetics [42]. Conjugation of 11 targeting peptides per nanoparticle resulted in greater than tenfold increase in fluorescence signal compared with a peptide-only control.

Fluorescent probes of metabolic activity

Alteration of cellular metabolism is one of the hallmarks of cancer [43]. Indeed, the use of ^{18}F -fluoro- D -glucose as a contrast agent for PET, is based on the increase in uptake of deoxyglucose associated with tumors. Fluorescently labeled fructose and deoxyglucose have been developed for *in vivo* optical imaging of cancer metabolism. Fructose labeled with 7-nitro-1,2,3-benzadiazole and Cy5.5 (1-Cy5.5-DF) were both shown to be taken up in breast

cancer cell lines; however, while the uptake of 7-nitro-1,2,3-benzadiazole was specific to GLUT5, a fructose transporter that is commonly expressed in cancers, that of 1-Cy5.5-DF was not [44]. Similar results were observed in studies with fluorescently labeled deoxyglucose. Uptake of 2-[N-(7-nitrobenz-2-oxa-1,3-diazol-4-yl)amino]-2-deoxy-D-glucose (2-NBDG) was specific to GLUT transporters and was competitively inhibited in the presence D-glucose. By contrast, uptake of Cy5.5-DG was not specific to the GLUT transporters [45]. Other studies have explored the use of topically delivered 2-NBDG in cell culture and excised normal and neoplastic human oral tissue. Neoplastic oral tissue was associated with higher uptake of the 2-NBDG, leading to a 3.7-fold increase in fluorescence signal compared with normal tissue [46]. A similar increase in fluorescence signal was observed in excised malignant breast tissue that was topically treated with 2-NBDG [47]. Sheth *et al.* investigated the use of iv. injected 2-NBDG to enhance fluorescence contrast of subcutaneously implanted tumors in mice; target-to-background ratios of approximately 3 were obtained with minimally invasive and intraoperative imaging [48].

Smart fluorescent probes

Image contrast using peptide- or antibody-targeted fluorescent dyes is limited primarily by two factors: the degree of differential biomarker expression associated with neoplastic tissue; and the degree of nonspecific labeling of tissues that do not express the targeted biomarker. One approach to improve image contrast is the use of 'smart fluorescent probes', which in an effort to reduce background signal, only fluoresce in the presence of a targeted biomarker. Generally consisting of a fluorophore and a quencher, such smart probes are designed such that the fluorophore and quencher are in sufficiently close physical proximity that fluorescence is quenched in the absence of a biomarker of interest. When present, the targeted biomarker induces a change in the smart contrast agent such that quenching no longer occurs and the contrast agent becomes fluorescent. This change in signal intensity is based on changes in conformation, chemical structure or displacement.

One class of smart probes is based on a fluorophore and quencher linked by a peptide sequence selected because it is cleaved by a protease of interest. In the absence of protease, such agents do not fluoresce due to self-quenching, while cleavage of the peptide linker induces fluorescence. A number of these fluorescent activateable probes are available commercially through PerkinElmer (MA, USA) for *in vivo* small animal imaging. A NIR probe selective for caspase-1 has been used to image apoptosis. In this example, multiple fluorophores are all linked to a poly-llysine backbone, each via a caspase-1 cleavable peptide sequence. On average, 18 fluorophores are conjugated to a single delivery molecule where they are in sufficiently close proximity to efficiently autoquench fluorescence. Cleavage of the peptide substrate results in a fluorescent signal [49]. Sheth *et al.* used the commercially available Prosense[®]750 (PerkinElmer), a protease-activated NIR dye, to improve the signal-to-background ratio of metastatic tumor foci in a murine xenograft model of peritoneal carcinomatosis by a minimum of 3.5-fold relative to white-light imaging [50]. Prosense680, a similar protease-activateable dye, was imaged *in vivo* to effectively monitor response of colon polyps to anti-TNF- α therapy in a murine model [51]. While initial results are encouraging, potential limitations of smart probes include slow uptake, low target-to-background ratios and uncertain specificity. In addition to protease-activatable imaging probes, smart probes designed to image pH, reactive oxygen species, hypoxia and other chemical changes are also available [52].

A second class of smart probes is based on the use of cell-penetrating peptides conjugated to fluorescent labels; cell-penetrating peptides such as polyarginine can efficiently deliver fluorescent cargo inside cells. Cell uptake can be blocked if the labeled cell-penetrating peptide is fused to an inhibitory domain containing negatively charged residues. Such fusions have led to a new class of activateable cell-penetrating peptides (ACPPs); in an

ACPP, the labeled cell-penetrating peptide is fused to an inhibitory domain via a peptide-cleavable linker. The linker is cleaved upon exposure to proteases, and the cell-penetrating peptide facilitates membrane binding and uptake in tumor cells in cell culture, in animal models and in resected human tumors [53,54]. Cultured cells labeled with ACPPs showed more than a tenfold increase in fluorescent signal upon linker cleavage; mice xenografted with human tumor cells secreting MMP-2 and -9 showed a two- to threefold increase in fluorescence relative to normal tissue. Conjugation of ACPPs to dendrimers improves iv. delivery of the contrast agent to the target by reducing uptake in skin, cartilage and kidney relative to free ACPPs. The ACPP dendrimers colocalized with the tumor and resulted in tenfold fewer residual tumor cells at the surgical site after image-guided surgery compared with surgery with no molecular imaging-based guidance. Fluorescence signal remaining after surgery was able to identify small pieces of residual tumor, which could be resected after the initial surgery, resulting in improved survival with ACPP dendrimer imaging guidance compared with standard surgery without guidance (Figure 3).

Molecular beacons are another class of smart fluorescent probes designed to image changes in gene expression. Molecular beacons consist of a short sequence of nucleic acid, complementary to the target mRNA to be detected, linking a fluorophore (donor) and a quencher in a particular conformation [55]. In the absence of target mRNA, the beacon is designed to self-hybridize in a stem-loop structure so that fluorescence is quenched. When the target mRNA is present, the beacon is designed so that kinetics favor hybridization to the target; hybridization induces a conformational change that results in a fluorescence signal. Due to the intracellular location of the target mRNA, the use of molecular beacons relies on being able to deliver contrast agent inside cells of interest. The simultaneous use of molecular beacons and antibody-targeted fluorescent dyes has recently been demonstrated to recognize mouse carcinoma stem cells; a beacon was designed to recognize Oct-4 mRNA, an intracellular transcription factor regulating differentiation, while an antibody-targeted dye was used to label SSEA-1, a cell surface protein specific to stem cells. Using the combination of dyes, undifferentiated stem cells could be distinguished from differentiated cells during flow cytometric analysis [56]. The combined detection of intracellular and surface protein markers appears to be a promising approach for highly sensitive and specific detection of neoplastic cells.

Nanoparticle-based contrast agents for molecular imaging

Plasmonic nanoparticles

Metallic nanoparticles, usually made of gold or silver, scatter light with remarkable efficiency by virtue of their strong surface plasmon resonance. The potential of metallic nanoparticles as optically interrogatable biological labels has led to the development of a variety of novel applications in bioanalytical chemistry with unprecedented sensitivity [57–64]. Typical scattering cross sections of metal nanoparticles greatly exceed the absorption cross-section of fluorescent dyes [65] and of fluorescent proteins [66,67]. The photostability, water solubility and nontoxicity of gold nanoparticles make these probes advantageous for biological imaging. Conjugation strategies to attach targeting or delivery moieties are well developed [68–71].

The development of gold nanoparticle-based contrast agents has given rise to new opportunities in optical imaging of cells and tissues; agents have been developed using gold-based nanoparticles with various geometries, including nanoshells [72–74], nanorods [75,76] and nanocages [77]. Gold nanoparticles can provide optical contrast via either absorption, scattering or luminescence; the surface plasmon resonance peak of gold nanoparticles is strongly influenced by particle size, shape, material composition and

interparticle spacing, and can be tuned to the NIR spectral region (700–850 nm), where tissue is the most transparent [78].

It has been demonstrated that targeted gold nanoparticles can be used to provide high contrast images of cancer cells using a variety of optical modalities to measure light scattered by the nanoparticles, including reflectance confocal microscopy [69,79], dark-field microscopy [80], phase-sensitive optical coherence tomography [81] and photoacoustic imaging [82,83].

The concept of plasmon coupling of gold nanoparticles has been explored extensively for molecular imaging of carcinogenesis [69,83,84]. A number of cancer-related targets exist as closely spaced hetero- and homodimers; EGFR is a prime example. Binding of the EGF ligand induces EGFR dimerization and receptor aggregation in the plasma membrane. Receptor mediated assembly of EGFR-targeted spherical gold nanoparticles on the cell membrane can result in a dramatic spectral shift of more than 100 nm [84]; this allows highly sensitive detection of labeled cells, even in the presence of single unbound gold bioconjugates. This plasmon coupling has also been used to monitor EGFR trafficking dynamics within the cell. Upon ligand binding, membrane-bound EGFR elicits growth-promoting signals; this signaling continues after internalization of activated receptor in early endosomes, ceasing after entry into lysosomes. As seen in Figure 4, the scattering spectrum of EGFR-targeted nanoparticles shifts from green to yellow to red as the receptor tracks from the cell membrane, to early endosomes and then to late endosomes/multivesicular bodies [85].

Composite nanoparticles can also provide contrast for optical imaging, as well as other traditional medical imaging modalities. Nanoroses are small nanoclusters, approximately 30 nm in diameter, composed of approximately 70 gold-coated iron oxide particles that display intense NIR absorbance. A dextran coating facilitates uptake by macrophages. The utility of dextran-coated nanoroses for imaging macrophages was explored in cell culture and in a rabbit model of atherosclerosis; nanorose-labeled and unlabeled macrophages could easily be distinguished using dark-field microscopy. Moreover, the strong NIR absorption coefficient of the nanoroses provides the potential for image-guided photoablation therapy [86]. Gold nanocages are hollow, porous nanostructures composed predominately of gold and created by reducing gold onto a silver nanocube template. Gold nanocages are typically less than 100 nm in size and have been explored as contrast agents for optical coherence tomography and photoacoustic tomography [87].

Gold nanorods exhibit intense two-photon luminescence, which can also provide a source of signal for optical imaging in tissue. Two-photon imaging of tissue phantoms treated with 50×15 nm gold nanorods functionalized with EGFR antibodies increased intensity by three orders of magnitude compared with cellular autofluorescence with 760 nm excitation [88].

Contrast agents based on gold nanoparticles have potential for *in vivo* use, with topical or systemic delivery. The inherent biocompatibility of gold implies that such agents can be used directly *in vivo* without the need for protective layer growth. In fact, long-term treatment of rheumatoid arthritis utilizing gold is performed without any deleterious bioeffects (dose of 1.2–1.8 g/year for >10 years) [89]. It has been estimated that between a few hundred micrograms and a few milligrams of gold would be required for a diagnostic procedure [69]. This is thousands of times less than the threshold for any side effects detected in clinical practice [90–92]. However, the *in vivo* toxicology of metallic nanoparticles is dependent on particle size, shape and surface chemistry [93]. Alternatively, other types of metallic nanoparticles may be used as optical contrast agents, but ease of synthesis and biocompatibility concerns are limiting factors. For example, silver

nanoparticles exhibit higher extinction coefficients and higher signal but are not as stable or biocompatible in comparison to gold nanoparticles [94].

Plasmonic nanoshells

Metallic nanoparticles with a dielectric core/metallic shell composition have been explored extensively as contrast agents for molecular imaging. In particular, the optical resonance of nanoshells with a silica core and thin gold coating can be tailored over a broad spectral range by simply changing the core size and the core-to-shell ratio. Optimizing nanoshells to have peak scattering in the NIR region imparts the highest imaging depth. The large optical cross-section of nanoshells is especially valuable for imaging modalities such as optical coherence tomography and confocal reflectance microscopy. Alternatively, for therapeutic purposes, nanoshells may be optimized to absorb light in this region for use in the photothermal ablation of cancers. Nanoshells targeted to HER2 have been used for dark-field and reflectance confocal imaging of HER2 positive human breast carcinoma cells *in vitro* and *ex vivo* human tissue sections [74,95,96]. NIR irradiation-induced heating of these antibody-targeted nanoshells resulting in photothermal ablation of cells bound to nanoparticles [74].

Nanoshell composition can be altered to reduce particle outer diameter while retaining peak scattering in the NIR. For example, gold–gold sulfide nanoparticles (40 nm) targeted to HER2, which are smaller than silica–gold nanoshells (120–150 nm), have also been used for photothermal ablation and multiphoton imaging [97]. Multilayer, composite spherical nanoparticles have been designed to further optimize optical properties for optical imaging and therapeutic purposes [71]. By altering the composition and thickness of three-layered nanospheres, ultra-sharp resonance peaks are possible, which could allow for multiple targets to be imaged simultaneously [71].

Semiconductor nanocrystals

Quantum dots are semiconductor nanocrystals with diameters smaller than the Bohr excitation diameter (2–10 nm). The size-dependent optical properties are due to quantum confinement of electrons and holes. Quantum dots also exhibit improved brightness due to their high extinction coefficients that are an order of magnitude higher than most fluorescent dyes. In addition, these particles have improved photostability compared with organic fluorophores, and their broad excitation bands and narrow emission spectra facilitate the simultaneous labeling of multiple biomarkers. Particle size and composition can be varied to achieve the desired emission properties. In addition, the need for an external excitation source may be eliminated with particular quantum dots.

To date, the use of traditional quantum dots containing cadmium selenide or cadmium sulfide for *in vivo* imaging has been limited to animal studies due to the toxicity of cadmium [98]. The clinical applicability of these agents is severely impeded by these toxicity concerns. Rare earth nanocrystals may serve as a biocompatible alternative to cadmium-based nanocrystals. Kumar *et al.* used a fluoride nanomatrix (NaYF₄, 20–30 nm) doped with rare-earth ions for optical imaging and MRI, respectively [99]. Particles were further modified with a targeting antibody, anti-CLAudin-4, to prove the targeting abilities [99,100]. Similarly, Y₂O₃ nanocrystals doped with fluorescent Eu³⁺ and paramagnetic gadolinium (Gd³⁺) and conjugated to folic acid were created through an all-aqueous wet-chemical process to yield a targeted, water soluble and biocompatible agent for *in vitro* testing [100]. Self-illuminating quantum dot conjugates were created by conjugating a mutant of the bioluminescent protein *Renilla reniformis* luciferase to carboxylate-presenting quantum dots. These particles are luminescent due to bioluminescent resonance energy transfer and have been used for *in vivo* imaging [101].

Multimodal contrast agents

While optical molecular imaging offers many benefits, one of its primary limitations is the relatively limited depth of penetration, especially in comparison with other molecular imaging modalities such as ultrasound and MRI. To address this limitation, several groups have designed targeted contrast agents that are active in multiple modalities, such as optical imaging and MRI [8,102–106]. Integrating multiple modalities can result in a technique that enables deep tissue imaging with a traditional imaging modality to identify suspicious areas, together with a companion optical modality to interrogate these suspicious regions with higher spatial resolution to more precisely determine tumor location, monitor systemic particle distribution or to improve surgical margin planning. The use of multimodal particles to track stem cells *in vivo* exemplifies how whole-body imaging using traditional modalities (MRI) can be combined with high-resolution optical imaging to provide new capabilities that may ultimately be useful to improve diagnosis or to monitor targeted therapeutics [107].

Magnetic resonance contrast agents may be classified according to whether they affect T_1 and T_2 relaxation times. For many multimodal probes, Gd is used for T_1 -weighted imaging and iron oxide is often used for T_2 -weighted imaging. For example, the use of gold-coated iron oxides for combined optical/ T_2 -weighted MRI was demonstrated by a number of groups [102–104]. In another example, mesoporous silicon was loaded with quantum dots and single-walled carbon nanotubes to enable optical imaging and MRI, respectively [105]. These mesoporous silicon containers facilitate transport of the contrast agents through the vascular system. ACPPs labeled with Cy5 and Gd have been combined to enable optical and T_1 -weighted MRI, respectively [106]. A single injection of ACPP dendrimers labeled with Cy5 and Gd enabled pre- and postoperative T_1 -weighted MRI, in addition to intraoperative fluorescence imaging [54].

More recent strategies have enabled the combination of traditional MRI together with both wide-field and high-resolution optical approaches. This is facilitated by the development of a nanoprobe composed of an iron oxide core with a dielectric polymer coating and a gold nanoshell, allowing for MRI, optical microscopy and photoacoustic imaging [108]. After conjugation to targeting ligands, these all-in-one nanostructures are envisioned for use in noninvasive imaging, molecular diagnosis and photothermal treatment of diseases such as cancer. The ability to use the same particle for multiple imaging techniques is advantageous due to the reduced amount of foreign material required, time saved and increased information made available.

Optical agents may also be combined with nuclear probes to create another class of multimodal imaging agents. Nuclear imaging modalities, such as PET and single photon emission computed tomography, enable whole-body imaging with high sensitivity. Similar sensitivities for optical and nuclear imaging allow for straightforward design and application of multimodal probes. The radioactive component of the agent may be used to provide data on probe biodistribution and clearance, while the optical component provides a clinician with the ability to visualize the target in real-time during surgical or endoscopic procedures. The addition of a positron-emitting radionuclide and a NIR fluorophore to trastuzumab (anti-HER2 antibody) allowed for identification of not only primary tumors but also metastases in a mouse model *in vivo* [109].

Delivery of molecular imaging agents

To obtain optical molecular images that reflect changes in biomarker expression requires the ability to deliver contrast agents to cells and tissues of interest, as well as the ability to wash away unbound contrast agent. Two primary routes of administration exist for delivery of imaging agents: topical application and iv. injection. Topical application is only appropriate

for certain epithelial tissues, but provides some distinct advantages in these cases. Typically, smaller amounts of contrast agent are required for topical application; this reduces potential toxicity and clearance concerns associated with *iv.* injection. However, achieving sufficient epithelial permeation of topically applied contrast agents is still a major barrier, especially for larger nanoparticle-based agents. Using *iv.* delivery can help enhance contrast agent accumulation in tumors via the enhanced permeability and retention effect. However, *iv.* delivery typically requires higher dosages of contrast agents and can lead to a higher nonspecific background signal.

The major barriers to delivery are shown in Figure 5. Topically applied contrast agents must permeate tight junctions in the epithelium and in some cases a tough, protective keratinized epithelium further hampers delivery. By contrast, agents administered through *iv.* injection must evade degradation and the immune system to reach the target organ. These *iv.* agents must then localize to the area of interest and leave the circulatory system by passing through endothelial tight junctions. If the *iv.* contrast agent targets epithelial cells, it must also be transported through any stromal barriers. In addition, cytoplasmic- and nuclear-targeted agents delivered via either mechanism must also traverse the cell and nuclear membranes, respectively, to reach the intended target.

The tight junctions of the epithelium serve as a barrier to exclude foreign agents, so crossing this delivery barrier is not trivial. Chemical permeation enhancers such as Triton™-X and modified chitosan have been used to improve permeation in excised tissues [110–112]. Alternatively, pulsed ultrasound has been used to enhance permeation of 20 nm particles into the core of MCF-7 breast cancer spheroids compared with those not exposed to ultrasound [113]. These results show the potential for increasing delivery of imaging and therapeutic agents to tumor tissue and the effect of particle properties on penetration. Thick keratinized surfaces are not affected by many permeation enhancers and alternatives are needed for topical delivery of contrast agents to keratinizing epithelial tissues.

Contrast agent design and modification is especially important for *iv.* agents, as they must evade the immune system and avoid degradation. Size, shape and surface chemistry are critical for effective delivery. Polyethylene glycol is commonly used to create ‘stealth’ particles that evade immune clearance. For delivery to tumors, *iv.* delivery can leverage contrast agent accumulation by utilizing the enhanced permeability and retention effect due to poorly formed capillary networks near the tumor. However, in early neoplasia, agents must traverse the robust vascular endothelium to reach the targeted neoplastic cells. Early epithelial neoplasias near the tissue surface may not be accessible through the vascular network at all.

Delivery to cytoplasmic and nuclear targets adds an additional level of complexity. Peptides are a popular tool to overcome these barriers as many of them are inspired by viral systems that have successfully evolved to overcome barriers to intracellular delivery. Cytosolic delivery of gold nanoparticles (20 nm) was accomplished by conjugating a targeting antibody against actin and a TAT-HA2 peptide sequence to the surface of the particle [70]. The actin antibody targets the nanoparticle to a specific structure in the cell, while the TAT portion of the peptide enables endocytosis of the particles, and HA2 disrupts the endosomal lipid membrane enabling endosomal escape to the cytosol. Kang *et al.* used the nuclear localization signal peptide to target gold nanoparticles to the nucleus, causing cytokinesis arrest and resulting in the apoptosis of cancer cells *in vitro* [114]. A nuclear localization signal was also used by Oyelere *et al.* to improve delivery to the nucleus *in vitro* [115]. However, these particular particles will probably face other barriers following *iv.* delivery. The size of these particles would hinder *iv.* delivery due to retention in the blood pool followed by uptake in the liver [116].

Conclusion

Cancer is the second greatest cause of mortality in the world. There are important unmet clinical needs, which include more effective techniques to screen the general population to identify individuals at high risk for harboring early disease, tools to detect early neoplastic lesions in patients at risk and approaches to more effectively guide treatment of these early lesions.

The optical molecular imaging systems and agents described in this review hold the potential to image the morphologic, functional and molecular properties of early neoplastic lesions with improved resolution over currently used clinical technologies. To date, a number of optical probes, ranging from organic fluorophores to plasmonic nanoparticles have been developed to fulfill this need and are at various stages of clinical translation. While the small size of organic fluorophores facilitates delivery of such dyes, they are subject to photobleaching and may not achieve sufficient target-to-background ratios for clinical utility. Smart fluorescent probes can improve the target-to-background ratio, but concerns regarding specificity and low target signals are barriers that must be overcome. Plasmonic nanoparticles and nanoshells and other nanoparticle-based imaging agents offer an attractive alternative to fluorescent dyes, due to the modifiable surface chemistry and the ease with which therapeutic modalities (e.g., photothermal ablation) can be combined. However, the comparatively large size of these particles presents an increased number of barriers to *in vivo* delivery. An important barrier to translation of all these agents is the challenge associated with obtaining regulatory approval necessary to initiate clinical testing. However, as new biomarkers continue to be discovered and validated, and low-cost, highly sensitive, multimodal optical imaging systems reach clinical application, there is a growing opportunity to evaluate whether targeted optical contrast agents can help meet the clinical needs of early cancer detection.

Future perspective

When appropriately validated, these technologies can impact current clinical practice in the short term, by facilitating screening for and early detection of cancer and its precursors at a time when treatment is most effective. Through early detection and guidance of therapy, optical molecular imaging of cancer has the potential to reduce cancer morbidity and mortality. Since these tools are low cost and portable they are capable of expanding access to cancer screening and early detection. At the same time, these techniques can be used to study the molecular processes associated with carcinogenesis *in vivo* in humans. In particular, they provide the ability to directly image the biology of invasion and to study the host response serially over time. This knowledge can be used to change future clinical practice. In the future, integrated optical molecular systems can be used alone, or in combination with more traditional imaging technologies, to identify lesions at high risk of progression based on molecular, functional and phenotypic markers. This knowledge can be used to select the most appropriate choice of therapeutic agent. Finally, the ability to image molecular features of neoplasia can be used to provide a rapid molecular assessment of response.

Executive summary

Molecular optical imaging

- Molecular optical imaging combines advances in optical imaging with targeted, optically active contrast agents to enable noninvasive, real-time monitoring of the molecular changes associated with cancer development and progression.

- Low-cost optical imaging systems are available to acquire optical molecular imaging with a wide range of fields of view and spatial resolution, spanning the whole organ to the subcellular levels.
- Targeted, optically active contrast agents enable optical imaging of many biomarkers of cancer, associated with the initiation, development and progression of neoplastic lesions.

Molecular markers & targeting

- Advances in biomarker discovery and validation have been used to identify targeting moieties to label cancer-specific targets.
- Antibodies, antibody fragments, peptides, aptamers and small molecules are being explored as potential targeting moieties for optically active contrast agents.

Fluorescent dyes

- Fluorescent dyes possess many attractive properties as optical labels for use in optical molecular imaging systems: they have a low molecular weight, high quantum yield, are relatively low cost and there are many conjugation protocols available to attach targeting moieties. However, the depth of tissue imaging that can be achieved using fluorescence-based contrast agents is one limitation.
- Fluorescently labeled glucose derivatives allow for high-resolution, real-time visualization of changes in cell metabolism.
- Smart fluorescent probes only produce signal in the presence of a target, thereby lowering nonspecific background and improving specificity.

Nanoparticles

- Metal nanoparticles can provide optical contrast via either absorption, scattering or luminescence.
- The surface plasmon resonance peak of gold nanoparticles is strongly influenced by particle size, shape, material composition and interparticle spacing. It can be tuned to the near-infrared spectral region.
- Nanoshells, comprised of a metal shell and dielectric core, can be tuned over a broad range by varying the core-to-shell ratio and overall particle size for imaging and photothermal ablation purposes.
- Rare earth nanocrystals provide a biocompatible alternative to traditional cadmium-based quantum dots.

Multimodal agents

- Multimodal agents have been developed to enable simultaneous imaging with traditional medical imaging modalities and optical modalities. Integration of multiple modalities can result in the ability to image deep tissue with a traditional imaging modality to identify suspicious areas; these areas can then be examined with higher spatial resolution to more precisely determine tumor location with a companion optical modality.

Delivery

- Two primary routes of administration exist for delivery of optical molecular imaging agents: topical application and intravenous injection.

- Both routes of administration are affected by major delivery barriers, which are obstacles to the translation of these technologies.
- Delivery of imaging agents to cytoplasmic and nuclear targets adds an additional level of complexity, but various peptides have improved intracellular delivery.

Acknowledgments

The authors acknowledge support from the NIH Bioengineering Research Partnership grant (R01 CA103830). A Hellebust is supported through the National Science Foundation Graduate Research Fellowship Program (Grant No. 0940902).

References

Papers of special note have been highlighted as:

- of interest
 - of considerable interest
1. Vieth M, Ell C, Gossner L, May A, Stolte M. Histological analysis of endoscopic resection specimens from 326 patients with Barrett's esophagus and early neoplasia. *Endoscopy*. 2004; 36(9): 776–781. [PubMed: 15326572]
 2. Yao SL, Lu-Yao GL. The science and art of prostate cancer screening. *J. Natl Cancer Inst*. 2011; 103(6):450–450. [PubMed: 21350220]
 3. Hanahan D, Weinberg RA. The hallmarks of cancer. *Cell*. 2000; 100(1):57–70. [PubMed: 10647931]
 4. Glunde K, Pathak A, Bhujwala Z. Molecular-functional imaging of cancer: to image and imagine. *Trends Mol. Med*. 2007; 13(7):287–297. [PubMed: 17544849]
 5. Hong WK, Sporn MB. Recent advances in chemoprevention of cancer. *Science*. 1997; 278(5340): 1073–1077. [PubMed: 9353183]
 6. Pomper MG. Molecular imaging: an overview. *Acad. Radiol*. 2001; 8(11):1141–1153. [PubMed: 11721814]
 7. Moore SG, Shenoy PJ, Fanucchi L, Tumej JW, Flowers CR. Cost-effectiveness of MRI compared with mammography for breast cancer screening in a high-risk population. *BMC Health Serv. Res*. 2009; 9:9. [PubMed: 19144138]
 8. Louie AY. Multimodality imaging probes: design and challenges. *Chem. Rev*. 2010; 110(5):3146–3195. [PubMed: 20225900] ▪▪ Overview of advances in multimodal imaging with a specific focus on the combination of optical imaging and MRI.
 9. Pierce MC, Javier DJ, Richards-Kortum R. Optical contrast agents and imaging systems for detection and diagnosis of cancer. *Int. J. Cancer*. 2008; 123(9):1979–1990. [PubMed: 18712733]
 10. Rajadhyaksha M, Grossman M, Esterowitz D, Webb RH, Anderson RR. *In vivo* confocal scanning laser microscopy of human skin: melanin provides strong contrast. *J. Invest. Dermatol*. 1995; 104(6):946–952. [PubMed: 7769264]
 11. Lane PM, Gilhuly T, Whitehead P, et al. Simple device for the direct visualization of oral-cavity tissue fluorescence. *J. Biomed. Opt*. 2006; 11(2) 024006.
 12. Frangioni JV. New technologies for human cancer imaging. *J. Clin. Oncol*. 2008; 26(24):4012–4021. [PubMed: 18711192]
 13. Weissleder R, Pittet MJ. Imaging in the era of molecular oncology. *Nature*. 2008; 452(7187):580–589. [PubMed: 18385732]
 14. Curvers WL, Singh R, Song L, et al. Endoscopic tri-modal imaging for detection of early neoplasia in Barrett's oesophagus: a multi-centre feasibility study using high-resolution endoscopy, autofluorescence imaging and narrow band imaging incorporated in one endoscopy system. *Gut*. 2008; 57(2):167–172. [PubMed: 17965067]

15. Lam S, Macaulay C, Leriche JC, Palcic B. Detection and localization of early lung cancer by fluorescence bronchoscopy. *Cancer*. 2000; 89(11):2468–2473. [PubMed: 11147629]
16. Park SY, Follen M, Milbourne A, et al. Automated image analysis of digital colposcopy for the detection of cervical neoplasia. *J. Biomed. Opt.* 2008; 13(1):4029.
17. Roblyer D, Richards-Kortum R, Sokolov K, et al. Multispectral optical imaging device for *in vivo* detection of oral neoplasia. *J. Biomed. Opt.* 2008; 13(2) 024019.
18. Poh CF, Ng SP, Williams PM, et al. Direct fluorescence visualization of clinically occult high-risk oral premalignant disease using a simple hand-held device. *Head Neck*. 2007; 29(1):71–76. [PubMed: 16983693]
19. East JE, Suzuki N, Saunders BP. Comparison of magnified pit pattern interpretation with narrow band imaging versus chromoendoscopy for diminutive colonic polyps: a pilot study. *Gastrointest. Endosc.* 2007; 66(2):310–316. [PubMed: 17643705]
20. Suzuki H, Saito Y. Autofluorescence and narrow-band imaging endoscopy for detecting early-staged cancer in Barrett's esophagus: a case report. *Jpn. J. Clin. Oncol.* 2008; 38(12):871–871. [PubMed: 19036854]
21. Van Den Broek FJC, Fockens P, Van Eeden S, et al. Endoscopic tri-modal imaging for surveillance in ulcerative colitis: randomised comparison of high-resolution endoscopy and autofluorescence imaging for neoplasia detection; and evaluation of narrow-band imaging for classification of lesions. *Gut*. 2008; 57(8):1083–1089. [PubMed: 18367559]
22. Luo S, Zhang E, Su Y, Cheng T, Shi C. A review of NIR dyes in cancer targeting and imaging. *Biomaterials*. 2011; 32(29):7127–7138. [PubMed: 21724249]
23. Mather S. Molecular imaging with bioconjugates in mouse models of cancer. *Bioconj. Chem.* 2009; 20(4):631–643.
24. Doubrovin M, Serganova I, Mayer-Kuckuk P, Ponomarev V, Blasberg RG. Multimodality *in vivo* molecular-genetic imaging. *Bioconj. Chem.* 2004; 15(6):1376–1388.
25. Hilger I, Leistner Y, Berndt A, et al. Near-infrared fluorescence imaging of HER-2 protein over-expression in tumour cells. *Eur. Radiol.* 2004; 14(6):1124–1129. [PubMed: 15118831]
26. Hsu ER, Anslyn EV, Dharmawardhane S, et al. A far-red fluorescent contrast agent to image epidermal growth factor receptor expression. *Photochem. Photobiol.* 2004; 79(3):272–279. [PubMed: 15115300]
27. Chang SK, Rizvi I, Solban N, Hasan T. *In vivo* optical molecular imaging of vascular endothelial growth factor for monitoring cancer treatment. *Clin. Cancer Res.* 2008; 14(13):4146–4153. [PubMed: 18593993]
28. Hoetker, MS.; Foersch, S.; Galle, PR.; Ralf, K.; Goetz, M. Digestive Disease Week. Chicago, IL, USA: 2011 May 7–10. Molecular *in vivo* imaging of gastrointestinal neoplasia with endomicroscopy using therapeutic antibodies against EGFR.
29. Foersch, S.; Kiesslich, R.; Hoetker, MS.; Galle, PR.; Neurath, MF.; Goetz, M. Digestive Disease Week. Chicago, IL, USA: 2011 May 7–10. *In vivo* immunohistochemistry with labeled bevacizumab using confocal laser endomicroscopy in models of human colorectal cancer.
30. Holliger P, Hudson PJ. Engineered antibody fragments and the rise of single domains. *Nat. Biotechnol.* 2005; 23(9):1126–1136. [PubMed: 16151406]
31. Lee S, Xie J, Chen X. Peptide-based probes for targeted molecular imaging. *Biochemistry*. 2010; 49(7):1364–1376. [PubMed: 20102226]
32. Reubi JC, Maecke HR. Peptide-based probes for cancer imaging. *J. Nucl. Med.* 2008; 49(11): 1735–1738. [PubMed: 18927341]
33. Nitin N, Rosbach KJ, El-Naggar A, Williams M, Gillenwater A, Richards-Kortum RR. Optical molecular imaging of epidermal growth factor receptor expression to improve detection of oral neoplasia. *Neoplasia*. 2009; 11(6):542–551. [PubMed: 19484143]
34. Ke S, Wen XX, Gurfinkel M, et al. Near-infrared optical imaging of epidermal growth factor receptor in breast cancer xenografts. *Cancer Res.* 2003; 63(22):7870–7875. [PubMed: 14633715]
35. Adams KE, Ke S, Kwon S, et al. Comparison of visible and near-infrared wavelength-excitable fluorescent dyes for molecular imaging of cancer. *J. Biomed. Opt.* 2007; 12(2) 024017.

36. Hsiung PL, Hardy J, Friedland S, et al. Detection of colonic dysplasia *in vivo* using a targeted heptapeptide and confocal microendoscopy. *Nature Med.* 2008; 14(4):454–458. [PubMed: 18345013]
37. Kelly K, Alencar H, Funovics M, Mahmood U, Weissleder R. Detection of invasive colon cancer using a novel, targeted, library-derived fluorescent peptide. *Cancer Res.* 2004; 64(17):6247–6251. [PubMed: 15342411]
38. Li M, Anastassiades CP, Joshi B, et al. Affinity peptide for targeted detection of dysplasia in Barrett's esophagus. *Gastroenterology.* 2010; 139(5):1472–1480. [PubMed: 20637198]
39. Kelly KA, Waterman P, Weissleder R. *In vivo* imaging of molecularly targeted phage. *Neoplasia.* 2006; 8(12):1011–1018. [PubMed: 17217618]
40. Newton JR, Kelly KA, Mahmood U, Weissleder R, Deutscher SL. *In vivo* selection of phage for the optical imaging of PC-3 human prostate carcinoma in mice. *Neoplasia.* 2006; 8(9):772–780. [PubMed: 16984734]
41. Cheng Z, Wu Y, Xiong ZM, Gambhir SS, Chen XY. Near-infrared fluorescent RGD peptides for optical imaging of integrin $\alpha(v)\beta 3$ expression in living mice. *Bioconj. Chem.* 2005; 16(6): 1433–1441.
42. Kelly KA, Setlur SR, Ross R, et al. Detection of early prostate cancer using a hepsin-targeted imaging agent. *Cancer Res.* 2008; 68(7):2286–2291. [PubMed: 18381435]
43. Hanahan D, Weinberg RA. Hallmarks of cancer: the next generation. *Cell.* 2011; 144(5):646–674. [PubMed: 21376230]
44. Levi J, Cheng Z, Gheysens O, et al. Fluorescent fructose derivatives for imaging breast cancer cells. *Bioconj. Chem.* 2007; 18(3):628–634.
45. Cheng Z, Levi J, Xiong ZM, et al. Near-infrared fluorescent deoxyglucose analogue for tumor optical imaging in cell culture and living mice. *Bioconj. Chem.* 2006; 17(3):662–669.
46. Nitin N, Carlson AL, Muldoon T, El-Naggar AK, Gillenwater A, Richards-Kortum R. Molecular imaging of glucose uptake in oral neoplasia following topical application of fluorescently labeled deoxy-glucose. *Int. J. Cancer.* 2009; 124(11):2634–2642. [PubMed: 19173294]
47. Langsner R, Middleton L, Sun J, et al. Wide-field imaging of fluorescent deoxy-glucose in *ex vivo* malignant and normal breast tissue. *Biomed. Opt. Express.* 2011; 2(6):1514–1523. [PubMed: 21698015]
48. Sheth RA, Josephson L, Mahmood U. Evaluation and clinically relevant applications of a fluorescent imaging analog to fluorodeoxyglucose positron emission tomography. *J. Biomed. Opt.* 2009; 14(6) 064014. • Details the use of a fluorescently labeled glucose analog for minimally invasive detection of neoplasia and intraoperative imaging.
49. Messerli SM, Prabhakar S, Tang Y, et al. A novel method for imaging apoptosis using a caspase-1 near-infrared fluorescent probe. *Neoplasia.* 2004; 6(2):95–105. [PubMed: 15140398]
50. Sheth RA, Upadhyay R, Stangenberg L, Sheth R, Weissleder R, Mahmood U. Improved detection of ovarian cancer metastases by intraoperative quantitative fluorescence protease imaging in a pre-clinical model. *Gynecol. Oncol.* 2009; 112(3):616–622. [PubMed: 19135233]
51. Gounaris E, Tung CH, Restaino C, et al. Live imaging of cysteine–cathepsin activity reveals dynamics of focal inflammation, angiogenesis, and polyp growth. *PLoS One.* 2008; 3(8):e2916. [PubMed: 18698347]
52. Kobayashi H, Choyke PL. Target-cancer-cell-specific activatable fluorescence imaging probes: rational design and *in vivo* applications. *Acc. Chem. Res.* 2011; 44(2):83–90. [PubMed: 21062101]
53. Jiang T, Olson ES, Nguyen QT, Roy M, Jennings PA, Tsien RY. Tumor imaging by means of proteolytic activation of cell-penetrating peptides. *Proc. Natl Acad. Sci. USA.* 2004; 101(51): 17867–17872. [PubMed: 15601762]
54. Nguyen QT, Olson ES, Aguilera TA, et al. Surgery with molecular fluorescence imaging using activatable cell-penetrating peptides decreases residual cancer and improves survival. *Proc. Natl Acad. Sci. USA.* 2010; 107(9):4317–4322. [PubMed: 20160097] • Provides an example of a multimodal imaging agent with cell-penetrating capabilities used to improve preoperative and intraoperative imaging.

55. Bao G, Rhee WJ, Tsourkas A. Fluorescent probes for live-cell RNA detection. *Annu. Rev. Biomed. Eng.* 2009; 11:25–47. [PubMed: 19400712] • Overview of RNA imaging in living cells with fluorescent probes.
56. Rhee WJ, Bao G. Simultaneous detection of mRNA and protein stem cell markers in live cells. *BMC Biotechnol.* 2009; 9:30. [PubMed: 19341452]
57. Nabiev IR, Morjani H, Manfait M. Selective analysis of antitumor drug interaction with living cancer cells as probed by surface-enhanced Raman spectroscopy. *Eur. Biophys. J.* 1991; 19(6): 311–316. [PubMed: 1915156]
58. Kneipp K, Haka AS, Kneipp H, et al. Surface-enhanced Raman spectroscopy in single living cells using gold nanoparticles. *Appl. Spectroscopy.* 2002; 56(2):150–154.
59. Nie S, Emory SR. Probing single molecules and single nanoparticles by surface-enhanced Raman scattering. *Science.* 1997; 275(5303):1102–1106. [PubMed: 9027306]
60. Elghanian R, Storhoff JJ, Mucic RC, Letsinger RL, Mirkin CA. Selective colorimetric detection of polynucleotides based on the distance-dependent optical properties of gold nanoparticles. *Science.* 1997; 277(5329):1078–1080. [PubMed: 9262471]
61. Yasuda R, Noji H, Yoshida M, Kinosita K Jr, Itoh H. Resolution of distinct rotational substeps by submillisecond kinetic analysis of F1-ATPase. *Nature.* 2001; 410(6831):898–904. [PubMed: 11309608]
62. Schultz S, Smith DR, Mock JJ, Schultz DA. Single-target molecule detection with nonbleaching multicolor optical immunolabels. *Proc. Natl Acad. Sci. USA.* 2000; 97(3):996–1001. [PubMed: 10655473]
63. Yguerabide J, Yguerabide EE. Resonance light scattering particles as ultrasensitive labels for detection of analytes in a wide range of applications. *J. Cell. Biochem. Suppl.* 2001; 37:71–81. [PubMed: 11842431]
64. Sonnichsen C, Reinhard Bjorn M, Liphardt J, Alivisatos AP. A molecular ruler based on plasmon coupling of single gold and silver nanoparticles. *Nat. Biotechnol.* 2005; 23(6):741–745. [PubMed: 15908940]
65. Yguerabide J, Yguerabide EE. Light-scattering submicroscopic particles as highly fluorescent analogs and their use as tracer labels in clinical and biological applications. *Anal. Biochem.* 1998; 262(2):137–156. [PubMed: 9750128]
66. Shaner NC, Steinbach PA, Tsien RY. A guide to choosing fluorescent proteins. *Nat. Methods.* 2005; 2(12):905–909. [PubMed: 16299475]
67. Patterson GH, Knobel SM, Sharif WD, Kain SR, Piston DW. Use of the green fluorescent protein and its mutants in quantitative fluorescence microscopy. *Biophys. J.* 1997; 73:2782–2790. [PubMed: 9370472]
68. Horisberger M, Rosset J, Bauer H. Colloidal gold granules as markers for cell surface receptors in the scanning electron microscope. *Experientia.* 1975; 31(10):1147–1149. [PubMed: 1107057]
69. Sokolov K, Follen M, Aaron J, et al. Real-time vital optical imaging of precancer using anti-epidermal growth factor receptor antibodies conjugated to gold nanoparticles. *Cancer Res.* 2003; 63(9):1999–2004. [PubMed: 12727808]
70. Kumar S, Harrison N, Richards-Kortum R, Sokolov K. Plasmonic nanosensors for imaging intracellular biomarkers in live cells. *Nano Letters.* 2007; 7(5):1338–1343. [PubMed: 17439187]
71. Chen K, Liu Y, Ameer G, Backman V. Optimal design of structured nanospheres for ultrasharp light-scattering resonances as molecular imaging multilabels. *J. Biomed. Opt.* 2005; 10(2) 024005.
72. Adler DC, Huang S-W, Huber R, Fujimoto JG. Photothermal detection of gold nanoparticles using phase-sensitive optical coherence tomography. *Optics Express.* 2008; 16(7):4376–4393. [PubMed: 18542535]
73. Hirsch LR, Stafford RJ, Bankson JA, et al. Nanoshell-mediated near-infrared thermal therapy of tumors under magnetic resonance guidance. *Proc. Natl Acad. Sci. USA.* 2003; 100(23):13549–13554. [PubMed: 14597719]
74. Loo C, Lowery A, Halas N, West J, Drezek R. Immunotargeted nanoshells for integrated cancer imaging and therapy. *Nano Letters.* 2005; 5(4):709–711. [PubMed: 15826113]

75. Huang X, El-Sayed IH, Qian W, El-Sayed MA. Cancer cell imaging and photothermal therapy in the near-infrared region by using gold nanorods. *J. Am. Chem. Soc.* 2006; 128(6):2115–2120. [PubMed: 16464114]
76. Pissuwan D, Valenzuela SM, Killingsworth MC, Xu X, Cortie MB. Targeted destruction of murine macrophage cells with bioconjugated gold nanorods. *J. Nanopart. Res.* 2007; 9(6):1109–1124.
77. Skrabalak SE, Chen J, Au L, Lu X, Li X, Xia Y. Gold nanocages for biomedical applications. *Adv. Mater.* 2007; 19(20):3177–3184. [PubMed: 18648528]
78. Larson T, Travis K, Joshi P, Sokolov K, Boas DA, Pitris CP, Ramanujam K. Nanoparticles for targeted therapeutics and diagnostics. *Handbook of Biomedical Optics*. 2011 London, UK Taylor & Francis:697–721. ■ Provides a detailed overview of nanoparticle-based agents with diagnostic and therapeutic value.
79. Aaron J, Nitin N, Travis K, et al. Imaging of epidermal growth factor receptor in early carcinogenesis using plasmon resonance coupling of metal nanoparticles. *J. Biomed. Opt.* 2007; 12(3) 034007.
80. El-Sayed IH, Huang X, El-Sayed MA. Surface plasmon resonance scattering and absorption of anti-EGFR antibody conjugated gold nanoparticles in cancer diagnostics: applications in oral cancer. *Nano Letters*. 2005; 5(5):829–834. [PubMed: 15884879]
81. Skala MC, Crow MJ, Wax A, Izatt JA. Photothermal optical coherence tomography of epidermal growth factor receptor in live cells using immunotargeted gold nanospheres. *Nano Letters*. 2008; 8(10):3461–3467. [PubMed: 18767886]
82. Yang XM, Skrabalak SE, Li ZY, Xia YN, Wang LHV. Photoacoustic tomography of a rat cerebral cortex *in vivo* with au nanocages as an optical contrast agent. *Nano Letters*. 2007; 7(12):3798–3802. [PubMed: 18020475]
83. Mallidi S, Larson T, Aaron J, Sokolov K, Emelianov S. Molecular specific optoacoustic imaging with plasmonic nanoparticles. *Optics Express*. 2007; 15(11):6583–6588. [PubMed: 19546967]
84. Aaron J, Nitin N, Travis K, et al. Plasmon resonance coupling of metal nanoparticles for molecular imaging of carcinogenesis *in vivo*. *J. Biomed. Opt.* 2007; 12(3) 034007.
85. Aaron J, Travis K, Harrison N, Sokolov K. Dynamic imaging of molecular assemblies in live cells based on nanoparticle plasmon resonance coupling. *Nano Letters*. 2009; 9(10):3612–3618. [PubMed: 19645464] ■ Details the use of gold nanoparticles for dynamic imaging of EGF receptor trafficking in live cells.
86. Ma LL, Feldman MD, Tam JM, et al. Small Multifunctional nanoclusters (nanoroses) for targeted cellular imaging and therapy. *ACS Nano*. 2009; 3(9):2686–2696. [PubMed: 19711944]
87. Skrabalak SE, Chen JY, Sun YG, et al. Gold nanocages: synthesis, properties, and applications. *Acc. Chem. Res.* 2008; 41(12):1587–1595. [PubMed: 18570442]
88. Durr NJ, Larson T, Smith DK, Korgel BA, Sokolov K, Ben-Yakar A. Two-photon luminescence imaging of cancer cells using molecularly targeted gold nanorods. *Nano Letters*. 2007; 7(4):941–945. [PubMed: 17335272]
89. Abrams MJ, Murrer BA. Metal compounds in therapy and diagnosis. *Science*. 1993; 261(5122): 725–730. [PubMed: 8102010]
90. Smith RW, Leppard B, Barnett NL, Millward-Sadler GH, McCrae F, Cawley MI. Chrysiasis revisited: a clinical and pathological study. *Br. J. Dermatol.* 1995; 133(5):671–678. [PubMed: 8555015]
91. Beckett VL, Doyle JA, Hadley GA, Spear KL. Chrysiasis resulting from gold therapy in rheumatoid arthritis: identification of gold by x-ray microanalysis. *Mayo Clin. Pro.* 1982; 57(12): 773–777.
92. Yun Patricia L, Arndt Kenneth A, Anderson RR. Q-switched laser-induced chrysiasis treated with long-pulsed laser. *Arch. Dermatol.* 2002; 138(8):1012–1014. [PubMed: 12164737]
93. Mahmoudi M, Azadmanesh K, Shokrgozar MA, Journeay WS, Laurent S. Effect of nanoparticles on the cell life cycle. *Chem. Rev.* 2011; 111(5):3407–3432. [PubMed: 21401073]
94. Javier DJ, Nitin N, Roblyer DM, Richards-Kortum R. Metal-based nanorods as molecule-specific contrast agents for reflectance imaging in 3D tissues. *J. Nanophotonics*. 2008; 2(1):23506. [PubMed: 19066632]

95. Loo C, Hirsch L, Lee MH, et al. Gold nanoshell bioconjugates for molecular imaging in living cells. *Optics Letters*. 2005; 30(9):1012–1014. [PubMed: 15906987]
96. Bickford LR, Agollah G, Drezek R, Yu TK. Silica-gold nanoshells as potential intraoperative molecular probes for HER2-overexpression in *ex vivo* breast tissue using near-infrared reflectance confocal microscopy. *Breast Cancer Res. Treat.* 2010; 120(3):547–555. [PubMed: 19418216]
97. Day ES, Bickford LR, Slater JH, Riggall NS, Drezek RA, West JL. Antibody-conjugated gold–gold sulfide nanoparticles as multifunctional agents for imaging and therapy of breast cancer. *Int. J. Nanomed.* 2010; 5:445–454.
98. Derfus AM, Chan WCW, Bhatia SN. Probing the cytotoxicity of semiconductor quantum dots. *Nano Letters*. 2004; 4(1):11–18.
99. Kumar R, Nyk M, Ohulchanskyy TY, Flask CA, Prasad PN. Combined optical and MR bioimaging using rare earth ion doped NaYF₄ nanocrystals. *Adv. Funct. Mater.* 2009; 19(6):853–859.
100. Setua S, Menon D, Asok A, Nair S, Koyakutty M. Folate receptor targeted, rare-earth oxide nanocrystals for bi-modal fluorescence and magnetic imaging of cancer cells. *Biomaterials*. 2010; 31(4):714–729. [PubMed: 19822364]
101. So MK, Xu CJ, Loening AM, Gambhir SS, Rao JH. Self-illuminating quantum dot conjugates for *in vivo* imaging. *Nat. Biotechnol.* 2006; 24(3):339–343. [PubMed: 16501578]
102. Ji XJ, Shao RP, Elliott AM, et al. Bifunctional gold nanoshells with a superparamagnetic iron oxide-silica core suitable for both MR imaging and photothermal therapy. *J. Phys. Chem. C*. 2007; 111(17):6245–6251.
103. Larson TA, Bankson J, Aaron J, Sokolov K. Hybrid plasmonic magnetic nanoparticles as molecular specific agents for MRI/optical imaging and photothermal therapy of cancer cells. *Nanotechnology*. 2007; 18 325101.
104. Mahmoudi M, Serpooshan V, Laurent S. Engineered nanoparticles for biomolecular imaging. *Nanoscale*. 2011; 3(8):3007–3026. [PubMed: 21717012]
105. Tasciotti E, Liu XW, Bhavane R, et al. Mesoporous silicon particles as a multistage delivery system for imaging and therapeutic applications. *Nat. Nanotechnol.* 2008; 3(3):151–157. [PubMed: 18654487]
106. Olson ES, Jiang T, Aguilera TA, et al. Activatable cell penetrating peptides linked to nanoparticles as dual probes for *in vivo* fluorescence and MR imaging of proteases. *Proc. Natl Acad. Sci. USA*. 2010; 107(9):4311–4316. [PubMed: 20160077]
107. Mahmoudi M, Hosseinkhani H, Hosseinkhani M, et al. Magnetic resonance imaging tracking of stem cells *in vivo* using iron oxide nanoparticles as a tool for the advancement of clinical regenerative medicine. *Chem. Rev.* 2011; 111(2):253–280. [PubMed: 21077606]
108. Jin Y, Jia C, Huang S-W, O'Donnell M, Gao X. Multifunctional nanoparticles as coupled contrast agents. *Nat. Commun.* 2010; 1:41. [PubMed: 20975706]
109. Sampath L, Kwon S, Hall MA, Price RE, Sevic-Muraca EM. Detection of cancer metastases with a dual-labeled near-infrared/positron emission tomography imaging agent. *Transl. Oncol.* 2010; 3(5):U307–U371.
110. Ghosn B, Van De Ven AL, Tam J, et al. Efficient mucosal delivery of optical contrast agents using imidazole-modified chitosan. *J. Biomed. Opt.* 2010; 15(1) 015003.
111. Van De Ven AL, Adler-Storthz K, Richards-Kortum R. Delivery of optical contrast agents using Triton-X100, part 1: reversible permeabilization of live cells for intracellular labeling. *J. Biomed. Opt.* 2009; 14(2) 021012.
112. Van De Ven AL, Adler-Storthz K, Richards-Kortum R. Delivery of optical contrast agents using Triton-X100, part 2: enhanced mucosal permeation for the detection of cancer biomarkers. *J. Biomed. Opt.* 2009; 14(2) 021013.
113. Grainger SJ, Serna JV, Sunny S, Zhou Y, Deng CX, El-Sayed MEH. Pulsed ultrasound enhances nanoparticle penetration into breast cancer spheroids. *Mol. Pharm.* 2010; 7(6):2006–2019. [PubMed: 20957996]
114. Kang B, Mackey MA, El-Sayed MA. Nuclear targeting of gold nanoparticles in cancer cells induces DNA damage, causing cytokinesis arrest and apoptosis. *J. Am. Chem. Soc.* 2010; 132(5): 1517–1519. [PubMed: 20085324]

115. Oyelere AK, Chen PC, Huang XH, El-Sayed IH, El-Sayed MA. Peptide-conjugated gold nanorods for nuclear targeting. *Bioconj. Chem.* 2007; 18:1490–1497.
116. Longmire M, Choyke PL, Kobayashi H. Clearance properties of nano-sized particles and molecules as imaging agents: considerations and caveats. *Nanomedicine.* 2008; 3(5):703–717. [PubMed: 18817471]

Websites

201. American Cancer Society. Cancer facts and figures 2008. 2008. [www.cancer.org/acs/groups/content/@nho/documents/document/2008caffinalsecuredpdf.pdf](http://www.cancer.org/acs/groups/content/@nho/documents/document/2008cafffinalsecuredpdf.pdf)
202. Boyle, P.; Levin, B. World Cancer Report 2008. 2008. www.iarc.fr/en/publications/pdfs-online/wcr/2008
203. National Cancer Institute. The NCI strategic plan for leading the nation to eliminate the suffering and death due to cancer. 2006. http://strategicplan.nci.nih.gov/pdf/nci_2007_strategic_plan.pdf

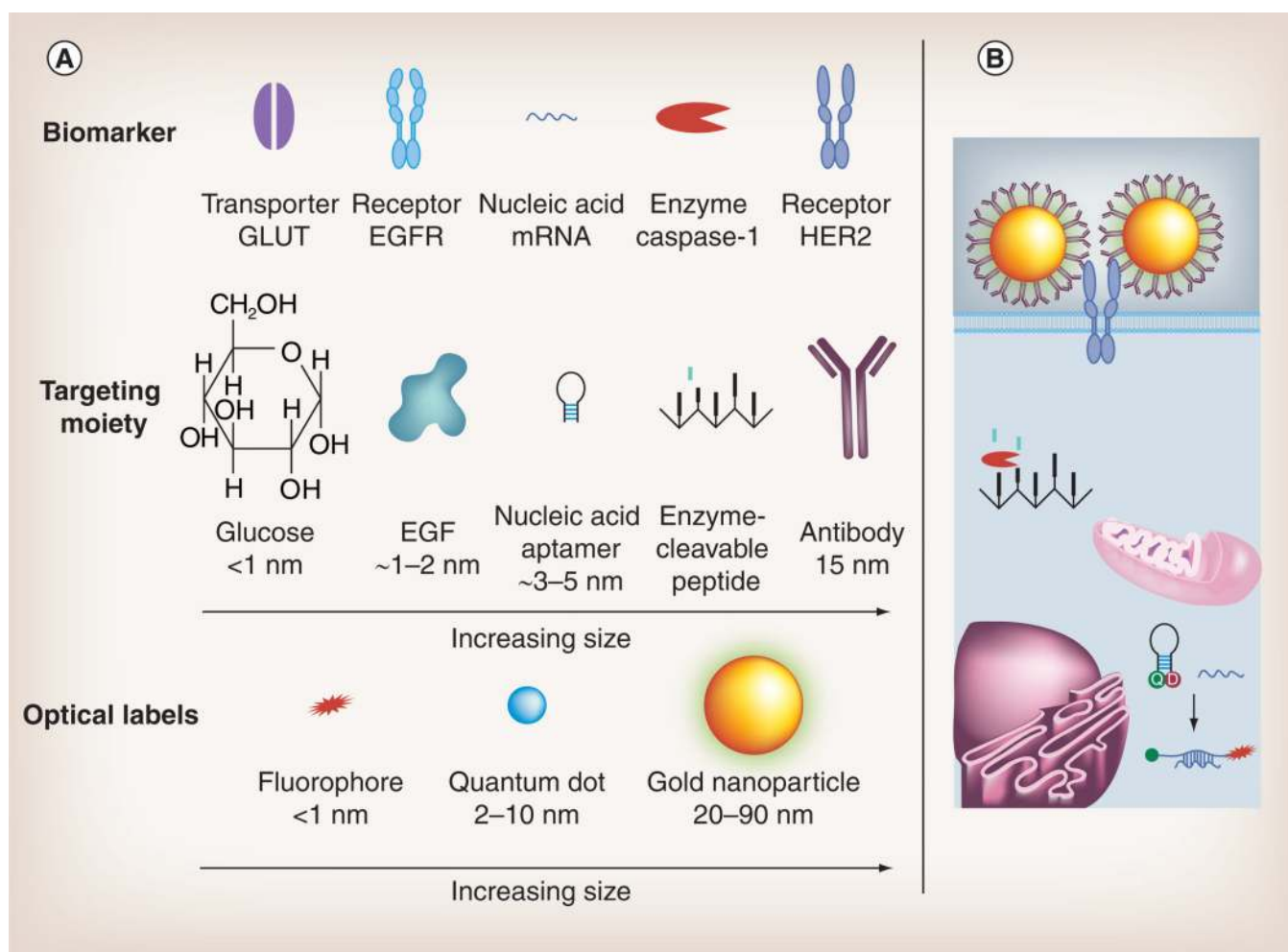


Figure 1. A variety of extra- and intracellular biomarkers serve as potential targets for contrast agents

(A) These biomarkers can be targeted with a wide range of targeting moieties, designed to maximize sensitivity and specificity. Optical labels, such as fluorophores, quantum dots and gold nanoparticles, can be conjugated to targeting moieties, to result in a strong source of optical signal for optical molecular imaging. (B) For example, antibody-targeted gold nanoparticles can be used to image *HER2* expression. Alternatively, an enzyme-cleavable peptide allows visualization of caspase-1 activity. Fluorescence from a nucleic acid aptamer is quenched until binding to the target mRNA sequence occurs.

D: Donor; EGFR: EGF receptor; Q: Quencher.

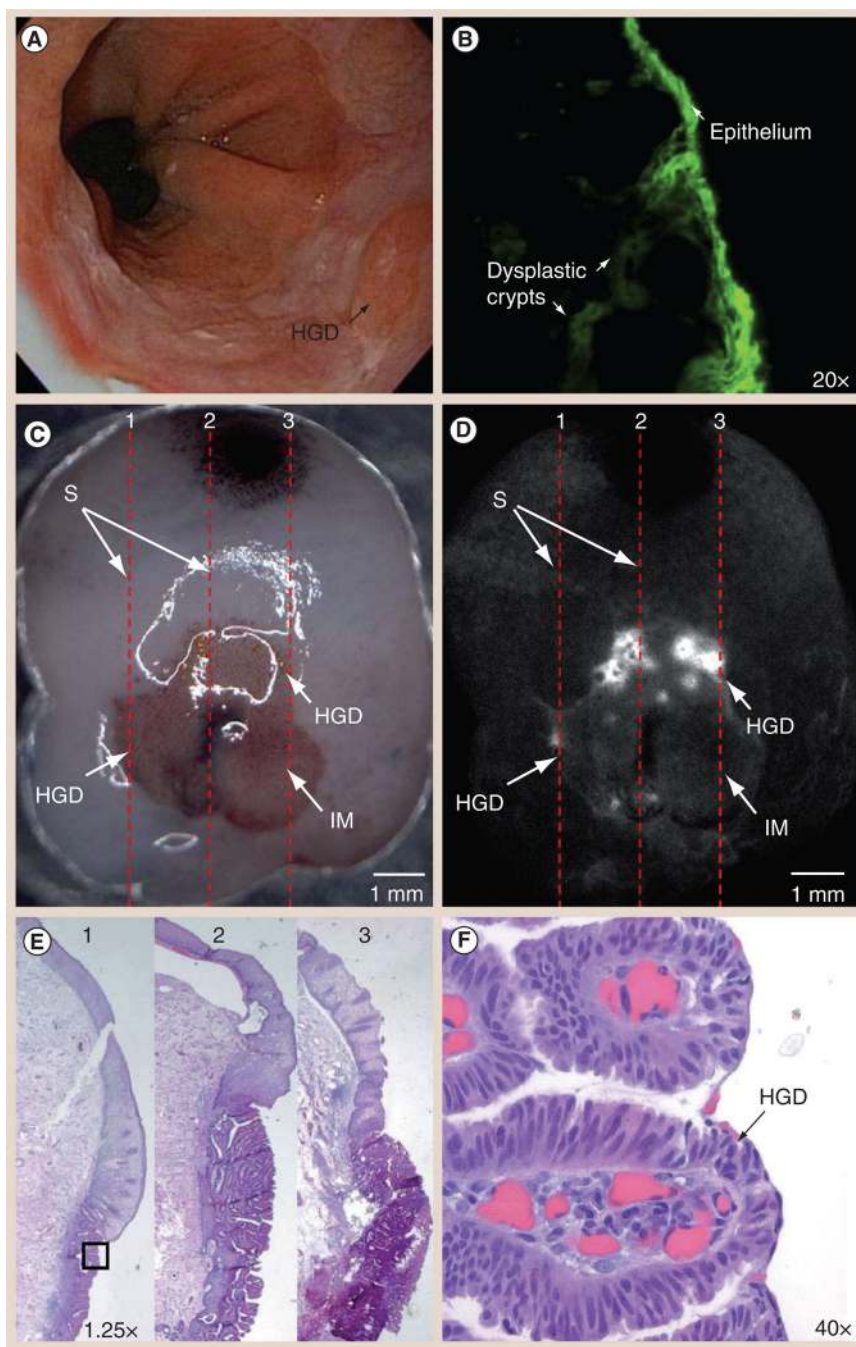


Figure 2. Peptide targeted contrast agent for the detection of dysplasia in Barrett's esophagus (A) A flat, focal area of HGD present in Barrett's esophagus on white light endoscopy. (B) A corresponding fluorescence image displays tissue labeled with peptide-targeted fluorescein isothiocyanate; areas of fluorescence correspond to subsurface dysplastic crypts. (C) Stereomicroscopy and (D) a corresponding fluorescence image of the resected specimen showing increased fluorescence intensity corresponding to regions of HGD, with minimal uptake in normal S regions or areas of IM. Histology from sections labeled 1–3 (red lines in (C–E)). (F) Magnified histologic view of HGD. Magnification: (B) 20 \times , (E) 1.25 \times and (F) 40 \times .

HGD: High-grade dysplasia; IM: Intestinal metaplasia; S: Squamous. Reproduced with permission from [38].

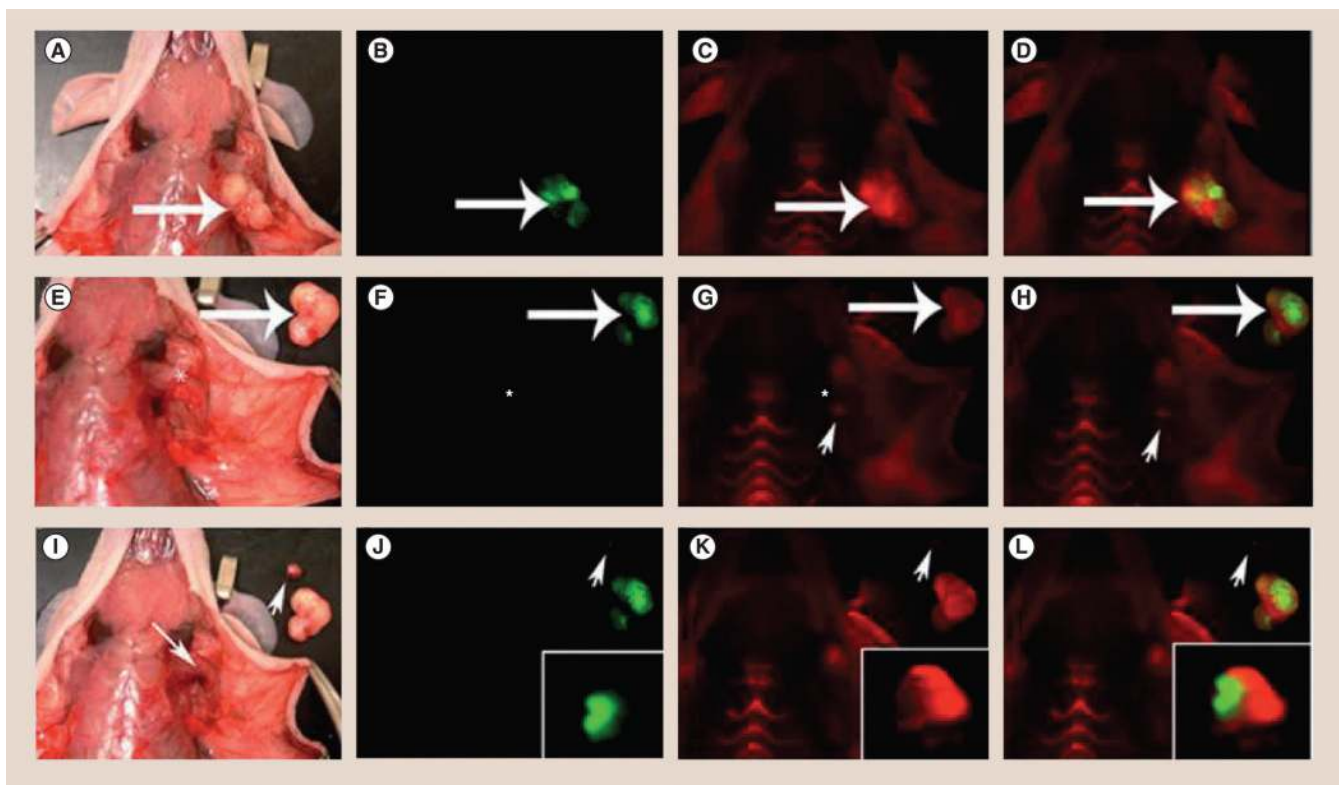


Figure 3. Activateable cell-penetrating peptides delineate residual tumor in the surgical margin (A–D) Activateable cell-penetrating peptides labeled with Cy5 delineate a green fluorescent protein-expressing MDA-MB 435 xenograft (large arrows) in the tumor bed. **(E & F)** Following excision, the tumor bed appears to be tumor free (*) under white light and GFP signal. **(G & H)** However, the Cy5 channel identifies residual fluorescence signal (small arrows) in the surgical margin. **(I)** Using Cy5 to guide resection, a small piece of residual tumor is identified under the muscle. **(J–L)** The residual tumor is removed and clear surgical margins confirmed by the green fluorescent protein and Cy5 channels. **(J–L)** Insets depict the excised residual tumor magnified and brightened $\times 5$.
Reproduced with permission from [54].

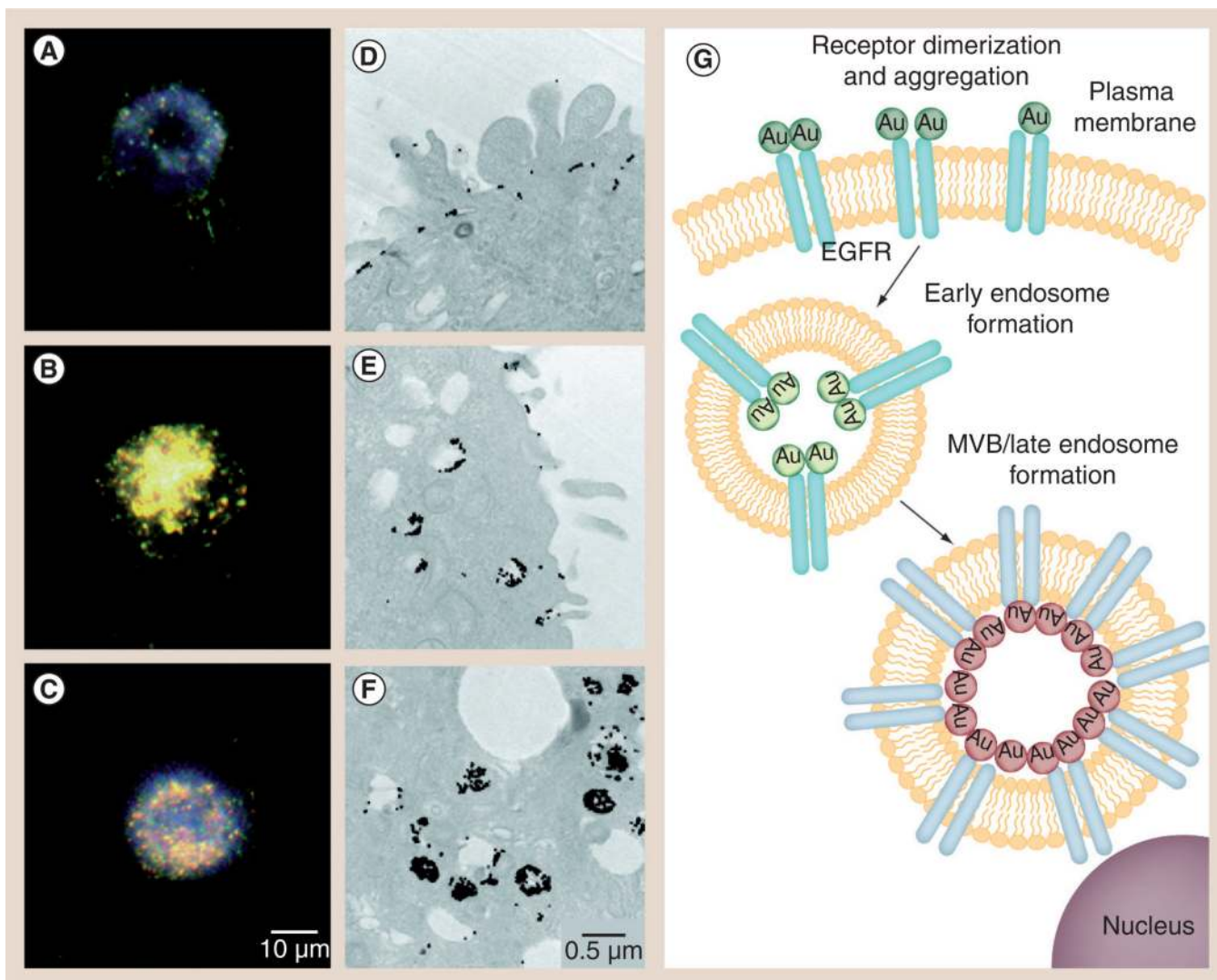


Figure 4. Gold nanoparticles for dynamic imaging of EGF receptor trafficking in live cells

Dark-field and transmission electron microscopy images of cells labeled with 25-nm anti-EGF receptor (EGFR)-targeted gold nanoparticle conjugates at (A & D) 4°C, (B & E) 25°C and (C & F) 37°C. Labeling at these temperatures arrests the EGFR regulatory process at critical points, with receptors located on the cell membrane at 4°C, endosomal internalization at 25°C and MVB sorting at 37°C. (G) The relationship between EGFR regulation state and the optical signature of the gold nanoparticles in that arrangement. MVB: Multivesicular body.

Reproduced with permission from [85].

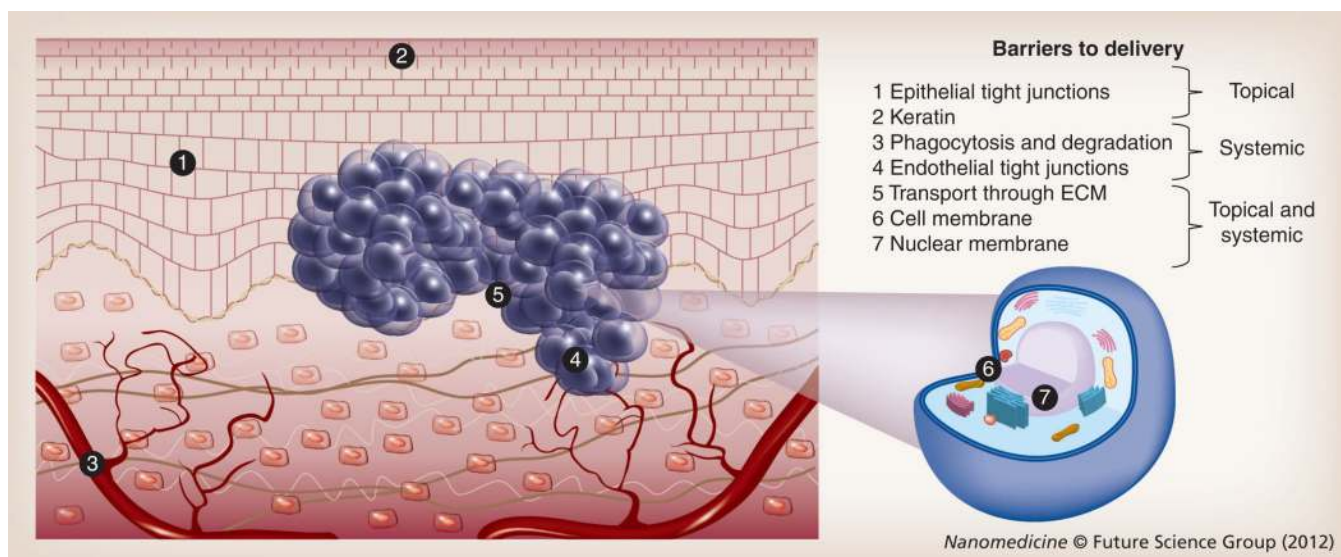


Figure 5. Barriers to contrast agent delivery

The two primary routes of administration for delivery of imaging agents are topical and systemic. Topically applied contrast agents must first permeate tight junctions in the epithelium (1) and in some cases a protective layer of keratin (2). Systemically administered contrast agents must evade degradation and the immune system to reach the target organ (3) and pass through endothelial tight junctions to leave the circulatory system (4). If the contrast agent targets epithelial cells, transportation through stromal barriers is necessary (5). Regardless of administration route, cell (6) and nuclear membranes (7) must be traversed by cytoplasmic- and nuclear-targeted agents, respectively. ECM: Extracellular matrix.